

REPORT DOCUMENTATION PAGE			Form Approved OMB NO. 0704-0188	
<p>The public reporting burden for this collection of information is estimated to average 1 hour per response, including the time for reviewing instructions, searching existing data sources, gathering and maintaining the data needed, and completing and reviewing the collection of information. Send comments regarding this burden estimate or any other aspect of this collection of information, including suggestions for reducing this burden, to Washington Headquarters Services, Directorate for Information Operations and Reports, 1215 Jefferson Davis Highway, Suite 1204, Arlington VA, 22202-4302. Respondents should be aware that notwithstanding any other provision of law, no person shall be subject to any penalty for failing to comply with a collection of information if it does not display a currently valid OMB control number.</p> <p>PLEASE DO NOT RETURN YOUR FORM TO THE ABOVE ADDRESS.</p>				
1. REPORT DATE (DD-MM-YYYY)		2. REPORT TYPE		3. DATES COVERED (From - To)
		New Reprint		-
4. TITLE AND SUBTITLE			5a. CONTRACT NUMBER	
Role of electrostatic interactions in two-dimensional self-assembly of tobacco mosaic viruses on cationic lipid monolayers			W911NF-09-1-0236	
			5b. GRANT NUMBER	
			5c. PROGRAM ELEMENT NUMBER	
6. AUTHORS			5d. PROJECT NUMBER	
Suntao Wang, Masafumi Fukuto, Antonio Checco, Zhongwei Niu, Qian Wang, Lin Yang				
			5e. TASK NUMBER	
			5f. WORK UNIT NUMBER	
7. PERFORMING ORGANIZATION NAMES AND ADDRESSES			8. PERFORMING ORGANIZATION REPORT NUMBER	
University of South Carolina Research Foundatio South Carolina Research Foundation 901 Sumter ST, 5th floor Byrnes Columbia, SC 29208 -0001				
9. SPONSORING/MONITORING AGENCY NAME(S) AND ADDRESS(ES)			10. SPONSOR/MONITOR'S ACRONYM(S)	
U.S. Army Research Office P.O. Box 12211 Research Triangle Park, NC 27709-2211			ARO	
			11. SPONSOR/MONITOR'S REPORT NUMBER(S)	
			56056-CH.10	
12. DISTRIBUTION AVAILABILITY STATEMENT				
Approved for public release; distribution is unlimited.				
13. SUPPLEMENTARY NOTES				
The views, opinions and/or findings contained in this report are those of the author(s) and should not be construed as an official Department of the Army position, policy or decision, unless so designated by other documentation.				
14. ABSTRACT				
We explore two-dimensional self-assembly of tobacco mosaic viruses (TMVs) on a substrate-supported, fluid lipid monolayer by manipulating the electrostatic interactions, with specific focus on the effects of the cationic lipid concentration in the monolayer and the presence of Ca ²⁺ ions in the surrounding bulk solution. The TMV assemblies were characterized by grazing-incidence X-ray scattering and atomic force microscopy, and the inter-particle interaction quantified through X-ray scattering data analysis. In the absence of Ca ²⁺ ions, we found				
15. SUBJECT TERMS				
TMV; Self-assembly; 2D ordered array; X-ray scattering; Atomic force microscopy; Substrate-supported lipid membrane				
16. SECURITY CLASSIFICATION OF:			17. LIMITATION OF ABSTRACT	
a. REPORT	b. ABSTRACT	c. THIS PAGE	UU	
UU	UU	UU		
			15. NUMBER OF PAGES	
			19a. NAME OF RESPONSIBLE PERSON	
			Qian Wang	
			19b. TELEPHONE NUMBER	
			803-777-8436	

Report Title

Role of electrostatic interactions in two-dimensional self-assembly of tobacco mosaic viruses on cationic lipid monolayers

ABSTRACT

We explore two-dimensional self-assembly of tobacco mosaic viruses (TMVs) on a substrate-supported, fluid lipid monolayer by manipulating the electrostatic interactions, with specific focus on the effects of the cationic lipid concentration in the monolayer and the presence of Ca^{2+} ions in the surrounding bulk solution. The TMV assemblies were characterized by grazing-incidence X-ray scattering and atomic force microscopy, and the inter-particle interaction quantified through X-ray scattering data analysis. In the absence of Ca^{2+} ions, we found that higher charge densities on the lipid monolayer led to poorer in-plane order, which may be attributed to faster adsorption kinetics, due to the surface potential that increases with charge density. At the same time, higher lipid-charge densities also resulted in weaker repulsion between TMVs, due to partial screening of Coulomb repulsion by mobile cationic lipids in the monolayer. The lipid-charge dependence was diminished with increasing concentration of Ca^{2+} ions, which also led to tighter packing of TMVs. The results indicate that Ca^{2+} ions strengthen the screening of Coulomb repulsion between TMVs and consequently enhance the role of attractive forces. Control experiments involving Na^{+} ions suggest that the attractive inter-TMV interaction has contributions from both the van der Waals force and the counter-ion-induced attraction that depends on ion valence.

REPORT DOCUMENTATION PAGE (SF298)
(Continuation Sheet)

Continuation for Block 13

ARO Report Number 56056.10-CH
Role of electrostatic interactions in two-dimensio ...

Block 13: Supplementary Note

© 2011 . Published in Journal of Colloid and Interface Science, Vol. 358 (2) (2011), (8 (2)). DoD Components reserve a royalty-free, nonexclusive and irrevocable right to reproduce, publish, or otherwise use the work for Federal purposes, and to authorize others to do so (DODGARS §32.36). The views, opinions and/or findings contained in this report are those of the author(s) and should not be construed as an official Department of the Army position, policy or decision, unless so designated by other documentation.

Approved for public release; distribution is unlimited.



Role of electrostatic interactions in two-dimensional self-assembly of tobacco mosaic viruses on cationic lipid monolayers

Suntao Wang^{a,1}, Masafumi Fukuto^{b,*}, Antonio Checco^b, Zhongwei Niu^c, Qian Wang^c, Lin Yang^{a,*}

^a National Synchrotron Light Source, Photon Sciences Directorate, Brookhaven National Laboratory, Upton, NY 11973, United States

^b Condensed Matter Physics and Materials Science Department, Brookhaven National Laboratory, Upton, NY 11973, United States

^c Department of Chemistry and Biochemistry and Nanocenter, University of South Carolina, Columbia, SC 29208, United States

ARTICLE INFO

Article history:

Received 13 January 2011

Accepted 12 March 2011

Available online 21 March 2011

Keywords:

TMV

Self-assembly

2D ordered array

X-ray scattering

Atomic force microscopy

Substrate-supported lipid membrane

ABSTRACT

We explore two-dimensional self-assembly of tobacco mosaic viruses (TMVs) on a substrate-supported, fluid lipid monolayer by manipulating the electrostatic interactions, with specific focus on the effects of the cationic lipid concentration in the monolayer and the presence of Ca^{2+} ions in the surrounding bulk solution. The TMV assemblies were characterized by grazing-incidence X-ray scattering and atomic force microscopy, and the inter-particle interaction quantified through X-ray scattering data analysis. In the absence of Ca^{2+} ions, we found that higher charge densities on the lipid monolayer led to poorer in-plane order, which may be attributed to faster adsorption kinetics, due to the surface potential that increases with charge density. At the same time, higher lipid-charge densities also resulted in weaker repulsion between TMVs, due to partial screening of Coulomb repulsion by mobile cationic lipids in the monolayer. The lipid-charge dependence was diminished with increasing concentration of Ca^{2+} ions, which also led to tighter packing of TMVs. The results indicate that Ca^{2+} ions strengthen the screening of Coulomb repulsion between TMVs and consequently enhance the role of attractive forces. Control experiments involving Na^+ ions suggest that the attractive inter-TMV interaction has contributions from both the van der Waals force and the counter-ion-induced attraction that depends on ion valence.

© 2011 Elsevier Inc. All rights reserved.

1. Introduction

Self-assembly into ordered structures has been widely studied because of the interests in utilizing controlled self-assembly for practical applications [1,2]. Self-assembly processes in general are complex and can be influenced by factors such as the properties of the building blocks themselves (e.g. monodispersity, shape), the interaction between them, and kinetic properties of the system (e.g. mobility, reversibility). In simplified model systems, it is often possible to control these factors individually and quantitatively characterize the resulted structure so that the influence of the control factor can be understood. For instance, the interaction between the building blocks can be modified by increasing the screening of the electrostatic repulsion, by introducing attraction through capillary [3–5] and depletion [6,7] forces, or by surface-functionalizing the building blocks so that they would selectively interact with each other [8,9].

Recently we reported on two-dimensional assemblies of tobacco mosaic viruses (TMVs) and the use of X-ray scattering to characterize the TMV–TMV interaction within the assemblies [10]. In this model system, the negatively charged TMVs are adsorbed on a substrate-supported, positively charged lipid monolayer at a bulk buffer solution–substrate interface. The electrostatic interaction between these charged rods can be controlled by adjusting the solution properties (e.g. pH and ionic strength), while the fluidity of the lipid monolayer gives the particle mobility that is necessary to assemble into ordered structures. Due to the rod-like shape (300 nm long and 18 nm in diameter) of TMV particles, the assemblies consist of TMVs that are oriented along the interface and aligned parallel to their neighbors (Fig. 1). Therefore we can model these assemblies as one-dimensional fluids that are characterized only by the lateral distances between neighboring TMVs, defined as d , while neglecting their orientations. An attractive attribute of this model system is that there exist theories that analytically describe the behavior of 1D fluids for several types of inter-particle interactions [11–13]. The approximation as 1D fluid therefore allowed us to fit the X-ray scattering data from the TMV assemblies based on these theoretical predictions. This approach provided a means to characterize the nature of the inter-particle interaction and to quantify the effects of external controls on the inter-particle interaction and ultimately the self-assembly process.

* Corresponding authors. Fax: +1 631 344 2739 (M. Fukuto), fax: +1 631 344 3238 (L. Yang).

E-mail addresses: fukuto@bnl.gov (M. Fukuto), lyang@bnl.gov (L. Yang).

¹ Present address: Physics Department, Cornell University, Ithaca, NY 14853, United States.

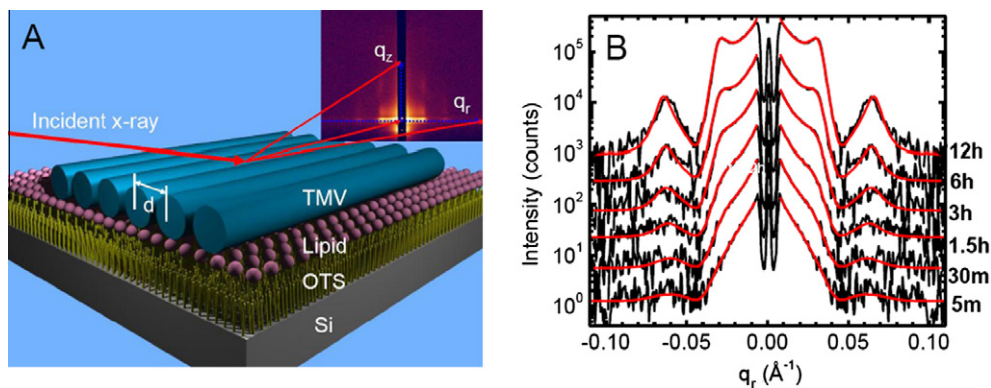


Fig. 1. (A) Schematic of a 2D TMV assembly and the sample geometry for GISAXS measurements. The q_z component of the scattering vector is along the sample normal while q_r is parallel to the sample surface. (B) Representative in-plane scattering intensity profiles along the surface enhance ridge (blue horizontal dashed line in A), as measured at a series of times after introducing TMVs into the bulk solution. The in-plane scattering data are analyzed by model fitting (red lines in B), as described in the text, to characterize the interaction between TMVs. (For interpretation of the references to color in this figure legend, the reader is referred to the web version of this article.)

The methods to tune the electrostatic interaction between charged building blocks include varying solution pH and ionic strength, which respectively control the net charge carried by each building block [14] and the screening of Coulomb repulsion between them [15]. The electrostatic interaction between TMVs can also depend on other parameters. For instance, our previous study provided evidence that the presence of Ca^{2+} ions gave rise to attraction between TMVs, based on the observation of increased TMV packing density and enhanced structural order in the assemblies. Others have also reported similar results in which highly ordered 2D structures were induced by multivalent ions [16,17].

Here, we explore this model system further by examining the effects of the lipid monolayer charge density and the Ca^{2+} concentrations on the formation of ordered TMV assemblies. Intuitively, one may expect higher monolayer charge density to promote TMV adsorption to achieve higher TMV density and perhaps better structural order. On the contrary, the present measurements in the absence of Ca^{2+} show that the structural order is actually poorer at higher lipid-charge density, likely due to faster TMV adsorption. Moreover, quantitative analysis of the grazing-incidence small-angle X-ray scattering (GISAXS) data demonstrates that increasing the lipid-charge density reduces the range of electrostatic repulsion between the adsorbed TMVs, possibly due to partial screening by the mobile cationic lipids (DOTAP) in the monolayer. On the other hand, under the 100 mM Ca^{2+} solution, the lipid-charge density is found to have little effect on the assembled TMV structures. Time-dependent measurements further show that the presence of Ca^{2+} ions reduces the rate of adsorption of TMV onto the lipid monolayer, which may also contribute to the better structural order in the TMV assemblies. The role of Ca^{2+} ions is further clarified by control experiments using solutions that have the same ionic strength but contain Na^+ ions instead. The TMV packing density under the Na^+ solution is found to be intermediate between the low-salt (pH buffer only) and Ca^{2+} -ion cases. The difference between the low-salt and high-salt (Na^+ or Ca^{2+} ions) results indicates that the van der Waals attraction, which does not depend on ion valence, likely contributes to facilitating the formation of better-ordered structures at high salt concentrations where the screening of electrostatic repulsion is strong. On the other hand, the difference between the Ca^{2+} and Na^+ results is evidence that counter-ion induced attraction, which depends on ion valence, also plays a role in the ordering of TMV assemblies. Our data therefore suggest a dual role of Ca^{2+} ions to provide screening to the Coulomb repulsion as well as to mediate attraction between TMVs.

2. Experimental methods

Sample preparation and data collection were performed following previously reported procedures [10,18], as briefly described below. The lipid monolayers of mixed dioleoylphosphatidylcholine (DOPC) and 1,2-dioleoyl-3-trimethylammonium-propane (DOTAP) were formed on OTS-coated silicon substrates in a Teflon cell by incubating the substrate for ~ 30 min under a solution of lipid vesicles prepared by sonication. After incubation, the sample cell was rinsed thoroughly using the buffer solution to ensure that free vesicles were removed and that the bulk solution had the desired pH and salt concentration. TMVs were then added into the sample cell. GISAXS measurements (schematically shown in Fig. 1A) were performed at beam-lines X21 and X9 at NSLS, as the TMV assemblies formed on the lipid monolayer. The structure became stable after 6–14 h, and the sample cell was rinsed again before a final GISAXS pattern was recorded. Atomic force microscopy measurements were performed on an Agilent 5500 AFM in the non-contact tapping mode using Olympus TR400PSA cantilevers (nominal stiffness ~ 0.08 N/m, resonance frequency ~ 15 kHz in water). The samples were prepared following the same procedure but in the AFM liquid sample cell. Only the final structure was measured using AFM, after rinsing the sample cell to remove non-adsorbed TMVs.

While the interpretation of AFM images is usually straightforward, the X-ray scattering data require non-trivial analysis. Following our previous study [10], we limit our analysis to the in-plane scattering profile near $q_z = 0$, and approximate the TMVs as parallel rods interacting via either exclusively hard-wall repulsion (hard rod model) or hard-wall repulsion with a short-ranged attraction (sticky rod model). As we have previously described in detail [10], this analysis approach permits structural characterization of TMV assemblies in terms of the packing fraction η of the rods, the hard-wall radius σ and, in the case of sticky rod model, the stickiness parameter α , which reflects the strength of the attractive potential well. These parameters provide the basis for evaluating how electrostatic interactions affect structural order within the TMV assemblies. Clearly, the hard rod and sticky rod interactions are only approximations of the overall interaction between the TMVs, which may contain contributions of various origins (e.g. screened Coulomb repulsion, van der Waal force and counter-ion-mediated attraction), as we will discuss below. Therefore the dependence of these simplified parameters provides a semi-quantitative description of how the TMV–TMV interactions are controlled by external parameters. But the numerical value of these parameters, for instance the hard-wall radius σ , may not

directly correspond to any physical characteristic of the TMVs (i.e. the diameter of the TMV).

3. Results and discussion

In general structural order in 2D depends on the particle density and the inter-particle interaction, both of which can in principle be influenced by the electrostatic interactions between neighboring TMVs and those between the TMV and the lipid monolayer. In Section 1, we delineate how the charge density in the lipid monolayer affects the TMV-monolayer and inter-TMV interactions and the assembly of TMVs under low-salt conditions (10 mM MES buffer only to maintain the pH in the solution). In Section 2, we describe how the presence of 100 mM Ca^{2+} ions alters the TMV-monolayer interaction and diminishes the assembly's dependence on the cationic lipid concentration. In Section 3, we examine the role of Ca^{2+} ions further by discussing the results of additional measurements at a series of Ca^{2+} concentrations and those in the presence of Na^+ ions.

3.1. Effects of lipid monolayer charge density on TMV assembly in the absence of Ca^{2+}

We collected GISXS data from TMV assemblies under a 10 mM MES solution at pH 6.0 at a series of mole fraction, X_{TAP} , for the cationic DOTAP lipid in the monolayer. The measured in-plane scattering intensity, recorded when the TMV assemblies have become stable at 6–14 h after the injection of TMVs, are summarized in Fig. 2A. Clearly, the details of the q_r -dependent intensity modulations in the data vary with the lipid composition. In particular, as the DOTAP fraction is reduced (X_{TAP} from 1 to 0.048), the broad shoulder-like feature at $q_r < 0.03 \text{ \AA}^{-1}$ shifts to lower q_r and develops into a better defined peak. This behavior suggests that the decrease in the lipid-charge density tends to both reduce the local packing density and extend the range of the positional correlations between aligned TMVs. In the case of the neutral lipid monolayer ($X_{\text{TAP}} = 0$), the GISAXS data (not shown) displays no intensity modulations that are indicative of inter-TMV correlations, suggesting no significant TMV adsorption in the absence of cationic lipids.

In the absence of multivalent cations, the inter-TMV interactions are likely dominated by the screened Coulomb repulsion. We have previously shown [10], and confirm further in Fig. 2A, that the model fitting (solid lines) based on hard-wall repulsion adequately capture the salient features of the observed in-plane scattering profiles (symbols). The corresponding best-fit curves for $S(q_x\sigma)$ and the pair correlation functions $g(x/\sigma)$ are shown in Fig. S1 in Supporting information. Note that the packing fraction η is based on the effective diameter of the hard rod, which is greater than the TMV diameter because we approximated the longer-ranged electrostatic repulsion between TMVs as simple hard-wall repulsion. Therefore, instead of η , we utilize the ratio η/σ (Fig. 2C) as a better measure of the TMV packing density within aligned domains ($\sim 1/d$).

3.1.1. Cationic lipids contribute to the screening of repulsion between TMVs

The most notable trend in Fig. 2A and C is that the range of repulsion between TMVs decreases as the cationic lipid fraction in the monolayer is increased. Specifically, as the DOTAP fraction is raised from 5% to 100%, the GISAXS-extracted σ is found to decrease monotonically by a factor of ~ 2 and approach the TMV diameter of 18 nm (Fig. 2C). This observed σ behavior may be attributed to stronger screening of the electrostatic inter-TMV repulsion at higher lipid-charge densities due to the DOTAP molecules acting as mobile cations confined in the plane of the monolayer.

The monolayer charge density is of the order of $e/A_l \times X_{\text{TAP}}$, where $A_l \sim 0.7 \text{ nm}^2/\text{lipid}$ [19], or $0.07\text{--}1.4 \text{ e/nm}^2$ for the DOTAP fraction of $X_{\text{TAP}} = 0.048\text{--}1$. On the other hand, the surface charge density on TMV (with diameter $D = 18 \text{ nm}$ and length $L = 300 \text{ nm}$) is estimated to be $Q/(\pi DL) < \sim 0.1 \text{ e/nm}^2$, based on previously reported values of the net charge per TMV in aqueous solutions ($Q < \sim 1800 \text{ e}$) [10,20,21]. Therefore, over most of the probed range of lipid compositions, the charge density on the lipid monolayer should far exceed that on the TMV surface. Consequently, as we will discuss further below, a significant amount of free, mobile charges, i.e., DOTAP and condensed counter-ions, are expected to be present at the lipid monolayer–solution interface, which should re-distribute upon the adsorption of TMVs to partially screen the electrostatic repulsion between the TMVs.

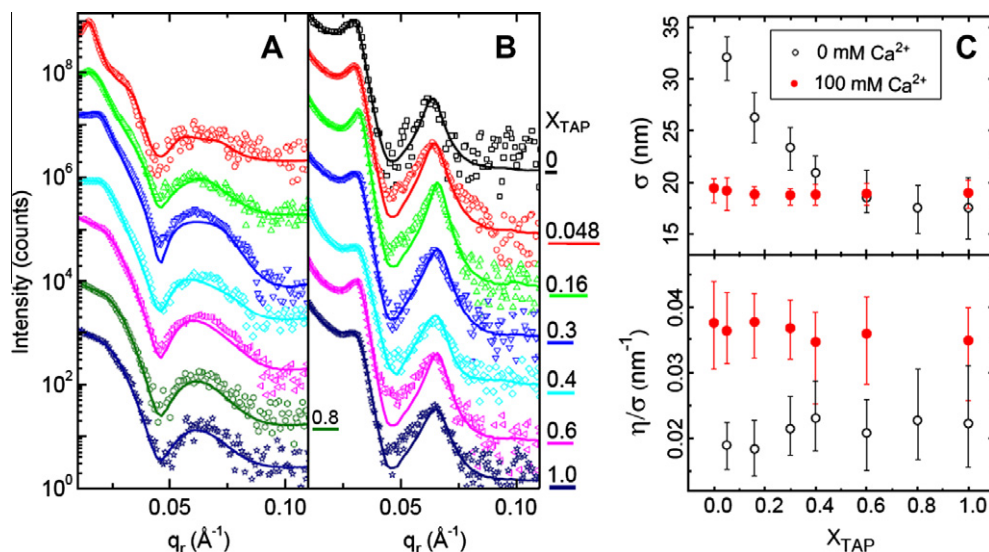


Fig. 2. The in-plane scattering profiles along the surface-enhanced ridge (see Fig. 1A) in the final scattering patterns from TMV assemblies adsorbed to substrate-supported DOPC/DOTAP monolayers under (A) Ca^{2+} -free MES buffers and (B) MES buffers that contain 100 mM Ca^{2+} . The mole fractions of DOTAP (X_{TAP}) in the corresponding lipid monolayers are listed beside the data. The data are shown as symbols, shifted vertically for clarity. The solid lines are the best-fits, based on the hard rod model for (A) and the sticky rod model for (B). The corresponding radius of hard-wall potential σ and packing density of rods η/σ are shown in (C).

This type of screening that is confined to the interface has been examined theoretically for the simple case of two infinitely long charged rods near the plane of a 2D salt solution by Menes et al. [22]. They found the potential energy for the inter-rod repulsion to be proportional to $(\lambda/d)^2$, where d is the spacing between rods and the effective screening length λ is inversely proportional to the charge density in the 2D salt. This is qualitatively consistent with the observed trend of decreasing TMV spacing with increasing lipid-charge density. We have previously estimated the net charge of each TMV to be $\sim -90 e$ [10]. This result was obtained by the Monte Carlo simulation based on the screened Coulomb repulsion between TMVs where the screening was assumed to arise from free ions in bulk solution only. The additional screening by mobile ions in 2D (i.e., DOTAP) may explain why the above estimated TMV charge is much lower than the often-cited value of $\sim -1800 e$ per TMV [20,21].

3.1.2. Density of adsorbed TMV weakly depends on lipid charge

The data in Fig. 2A and C also show that as the lipid-charge density is increased, the inter-TMV packing density, as measured by the ratio η/σ , only increases slightly. These GISAXS results are corroborated by AFM measurements. Representative AFM images of equilibrated TMV assemblies for $X_{\text{TAP}} = 0.16$, 0.4 and 1.0 are shown in Fig. 3, together with the corresponding GISAXS patterns. The tendency of the lipid-bound TMVs to pack closely and align locally is evident. Determined from measurements at 10 distinct locations in each AFM image, the average inter-TMV spacing is 39.5 ± 3.0 nm, 34.8 ± 2.2 nm and 32.7 ± 1.7 nm for $X_{\text{TAP}} = 0.16$, 0.4, and 1.0, respectively. The $\sim 20\%$ decrease in the AFM-derived inter-TMV spacing with increasing lipid-charge density is consistent with the $\sim 20\%$ increase in the best-fit values of the GISAXS-extracted η/σ over the same lipid composition range (black symbols, Fig. 2C).

The observed increase in the packing density of TMVs with increasing X_{TAP} agrees with the expectation that the adsorption of the anionic TMVs onto a cationic lipid monolayer is driven entropically by the counter-ion release mechanism [23–27]. The higher the lipid-charge density is, the greater number of counter-ions should be initially bound to the interface and hence can be released into the aqueous solution through the adsorption of macroions. Thus, the adsorption of TMVs is expected to increase with the lipid-charge density. This is consistent with the observations made in similar systems. Specifically, the 2D packing densities of anionic chains or rods in multi-lamellar polyelectrolyte–membrane complexes (DNA [25,26,28], α -helical polypeptides [29]) and polyelectrolytes adsorbed at membrane–solution interfaces (DNA [30],

polystyrene sulfonate [31]) were found to increase with the cationic lipid concentration.

However, the dependence of the inter-TMV spacing on the lipid-charge density that we observed is much weaker than that reported for those other 2D polyelectrolyte–lipid systems. Defining f to be the ratio between the multiplicative factors for the concomitant increases in $1/d$ and in the cationic lipid fraction, we obtain $f \sim 1.2/20 = 0.06$ (raising X_{TAP} from 0.048 to 1.0 leads to a $\sim 20\%$ increase in $1/d$ or $\sim \eta/\sigma$) for the 2D assemblies of TMVs. By contrast, the corresponding f values are higher by one order of magnitude for other charged rods: $f = 0.5$ – 0.8 for multi-lamellar DNA–lipid and polypeptide–lipid complexes [26,29], $f \sim 1$ for DNA adsorbed on cationic monolayers [30], and $f \sim 0.5$ for monolayer-bound polystyrene sulfonate [31].

This apparent discrepancy again may be explained by the overabundance of the cationic lipids in the monolayer. As discussed above, over most of the probed range of lipid compositions, the charge density on the lipid monolayer should far exceed that on the TMV surface ($< \sim 0.1 e/\text{nm}^2$). While the counter-ion release mechanism implies higher adsorption for weaker particle charge and higher monolayer charge density [14], adsorption is eventually limited by the electrostatic (and ultimately steric) repulsion between adsorbed particles. In addition, TMV's large size and surface curvature implies that the total area of the TMV–monolayer contacts should be much smaller than the total interfacial area. For these reasons, the interfacial assembly of TMVs is expected to release only a small fraction of the counter-ions that are originally associated with the cationic lipid monolayer. This may explain why the density of adsorbed TMVs does not strongly depend on the lipid-charge density. By contrast, with typical surface charge densities of 0.2 – $1.5 e/\text{nm}^2$ [27,29], the anionic rods are more highly charged in the multi-lamellar polyelectrolyte–lipid complexes, whose stability at low ionic strength relies on close matching of the charge densities on the polyelectrolyte and lipid–membrane surfaces [27,29].

3.1.3. Adsorption kinetics affects structural order

The AFM images in Fig. 3 further reveal that relatively large domains ($> \sim 1 \mu\text{m}$) of aligned TMVs are formed on the monolayer at $X_{\text{TAP}} = 0.16$ (Fig. 3A). By contrast, TMVs on the pure DOTAP monolayer ($X_{\text{TAP}} = 1.0$) form only small randomly-oriented “clusters” of five or fewer rods (Fig. 3C). The domain sizes observed at $X_{\text{TAP}} = 0.4$ (Fig. 3B) are intermediate between the above two cases. This apparent decrease in domain size with increasing lipid-charge density is qualitatively consistent with the GISAXS results, in which higher lipid-charge density results in a reduction in the modulation

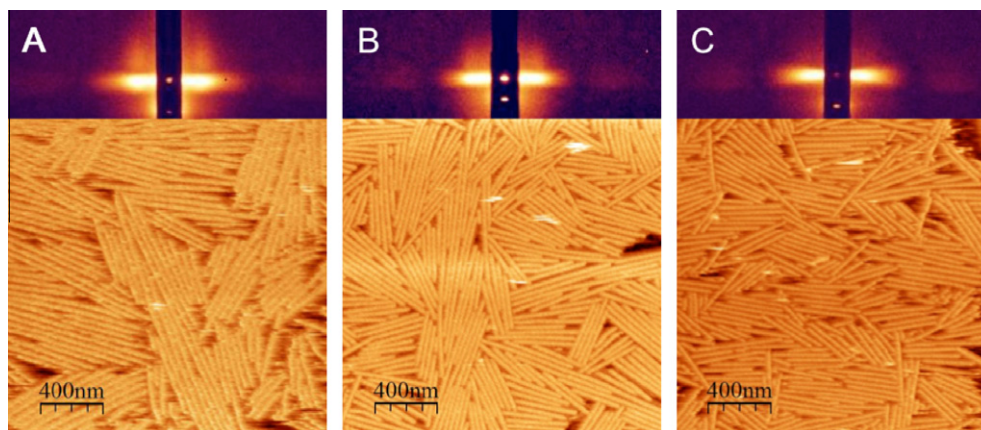


Fig. 3. GISAXS patterns and AFM images from three samples under Ca^{2+} -free 10 mM MES buffers with three different lipid monolayer compositions: $X_{\text{TAP}} = 0.16$ (A), 0.4 (B) and 1.0 (C).

amplitude of $S(q\sigma)$ (Fig. S1), indicating a greater degree of positional disorder in the TMV assembly.

The dependence of structural order in the TMV assemblies on lipid-charge density may be the consequence of the adsorption kinetics in the process of TMV self-assembly. Simple estimates based on the Grahame equation and the Gouy–Chapman theory [32] (Fig. S2) show that for the 10 mM MES solution at pH 6, raising the DOTAP fraction from 5% to 100% is expected to increase the interfacial potential by a factor of ~ 3.5 [$\psi(z=0) \sim 60 \rightarrow 210$ mV $\gg k_B T/e = 26$ mV], leading to a roughly two-fold enhancement in the potential at one Debye length away from the interface [$\psi(z=4.8$ nm) $\sim 20 \rightarrow 38$ mV]. Thus, an increase in the lipid-charge density should raise the adsorption rate by strengthening the electrostatic lipid–TMV attraction near the interface. The faster TMVs adsorbed, the less time would be allowed for the TMVs to freely diffuse and reorient themselves after adsorption. This in turn should induce the clustering of aligned rods at more sites and cause the resulting domains to be smaller. Therefore, the observed trend in the domain size is consistent with an increase in the adsorption rate at high lipid-charge densities.

3.1.4. Limitation of GISAXS measurements and analysis

While we did follow the formation of TMV assemblies with GISAXS as soon as TMVs were added into the buffer solution (e.g., Fig. 1B), our data did not conclusively show the above lipid-charge dependence of TMV adsorption kinetics. In Fig. 4A, the time dependence of the best fit η/σ is plotted for a few different lipid compositions. The results indicate that in the absence of Ca^{2+} , aligned domains of adsorbed TMVs started to form almost immediately after injection. However, the observed time evolution of η/σ did not show a definite systematic trend with varying lipid composition. This apparent discrepancy from the AFM results is likely due to the limited sensitivity of GISAXS to adsorption. The above AFM-based interpretation about the lipid-composition effect on the TMV adsorption rate refers to the earliest stage of the interfacial assembly. On the other hand, as shown in Fig. 4A, by the time the first set of analyzable GISAXS data was obtained, the local packing density ($\sim \eta/\sigma$) had already reached about a half of the final value. In view of this, a worthwhile extension of the present study would be to address the lipid-charge dependence of the adsorption rate more directly. Doing so will require experimental methods that are capable of finer time resolution and higher sensitivity to adsorption, such as quartz crystal microbalance with dis-

sipation (QCM-D) that has been utilized to quantify the formation of lipid bilayer on a substrate [33].

With the decreased domain sizes at high X_{TAP} , the hard rod model that approximates the TMV assemblies as 1D hard-wall fluid may no longer be adequate. This is mainly because the positional correlation between TMVs within each domain is now coupled with their orientations, which in turn are influenced by the presence of TMVs outside of the given domain. Furthermore, TMVs that do not belong to any ordered domains are expected to scatter X-rays as free particles (structure factor $S \sim 1$). With this contribution in the observed scattering intensity, the contrast of the TMV–TMV correlation peak would be reduced, causing the data to deviate from the line shape expected for a hard-wall fluid. The inadequacy of the hard rod model may partly explain the large error bars on the fitting parameters and why the extracted σ at the highest DOTAP concentrations falls slightly below the TMV diameter of 18 nm (Fig. 3A). However, this complication does not alter the main conclusions about the qualitative behavior of the lipid-charge dependence of the interaction between TMVs, namely, high X_{TAP} results in smaller average spacing between TMVs (higher packing density) but poorer positional order. These conclusions can be inferred directly from the position and width of the TMV–TMV correlation peak in the scattering data (see Fig. 2A and Fig. S3 in Supporting information).

3.2. Effect of lipid monolayer charge density on TMV assembly in the presence of 100 mM Ca^{2+}

Our previous study for $X_{\text{TAP}} = 0.16$ showed that the presence of Ca^{2+} ions enhanced the structural order within the TMV assemblies [10]. To find out how the Ca^{2+} ions would influence the lipid-charge dependence observed in Section 1, we carried out a similar set of experiments at various values of X_{TAP} using the solution that contained 100 mM Ca^{2+} ions (100 mM CaCl_2 , 10 mM MES, pH ~ 6.5). The observed scattering data are summarized in Fig. 2B. The best fits based on the sticky rod model (solid lines) reproduce the measured scattering profiles reasonably well. The corresponding $S(q_x\sigma)$ curves are shown in Fig. S1. The lipid-composition dependence of the extracted σ and η/σ is plotted as red solid symbols in Fig. 2C.

3.2.1. The screening of electrostatic interactions by Ca^{2+} ions reduces the lipid-charge dependence and growth rate of the TMV assembly

The data in Fig. 2B and C show that in the presence of Ca^{2+} both σ and η/σ are essentially independent of the lipid composition. Both the insensitivity of the assembled structure to the cationic lipid concentration and the near agreement between the best-fit hard-wall radius σ (~ 19 nm) and the TMV diameter (18 nm) are consistent with strong screening of the electrostatic inter-TMV repulsion that is expected for the 100 mM CaCl_2 solution (Debye length: $\kappa^{-1} = 0.6$ nm). Note that in contrast to the Ca^{2+} -free case (Section 1), ordered TMV structures formed on the pure DOPC monolayer in the presence of 100 mM Ca^{2+} ions. This may be due to charging of the monolayer as a result of Ca^{2+} ions binding to the phosphate moiety of the PC headgroup. Based on the reported binding constant of $K = 12\text{--}20$ M^{-1} [34], we estimate the surface charge density of the pure DOPC monolayer to be as high as $\sim 20\%$ of the value for the pure DOTAP monolayer (Fig. S4 in Supporting information).

Strong screening provided by Ca^{2+} ions also affects the growth of ordered domains. As shown in Fig. 4B, the time dependence of the best-fit η/σ indicates that the assembly develops rather slowly in the presence of Ca^{2+} , where it takes 2–3 h for the local packing density ($\sim \eta/\sigma$) to reach $\sim 50\%$ of the final values. This should be contrasted from the Ca^{2+} -free case (Fig. 4A), for which η/σ exceeds the 50% mark in less than ~ 1 h. The presence of 100 mM Ca^{2+} is

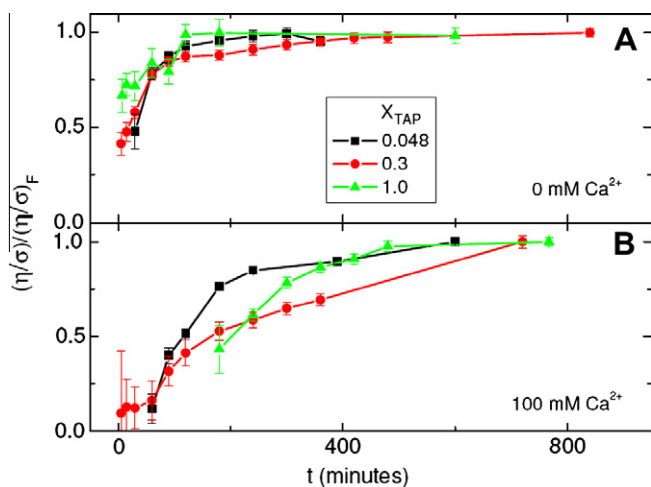


Fig. 4. Time dependence of the best-fit η/σ , normalized to the final value (η/σ_F), for three different lipid compositions under 10 mM buffer solutions that contain (A) 0 mM and (B) 100 mM CaCl_2 .

expected to significantly reduce the surface potential at the monolayer–solution interface (by a factor of ~ 2 ; see Figs. S2 and S4) and to cause the electrostatic TMV–lipid attraction to be much shorter ranged ($\kappa^{-1} = 0.6$ nm at 100 mM Ca^{2+} vs. 4.8 nm at 0 mM Ca^{2+}). All these effects should slow down the TMV adsorption and the growth of ordered domains and contribute, together with the Ca^{2+} -induced inter-TMV attraction to be discussed next, to reducing the influence of lipid compositions on the 2D assembly.

3.2.2. Attraction between TMVs is essential in forming the ordered assemblies induced by Ca^{2+}

As noted previously [10], a key result of the above analysis is that $S(q_x)$ for the Ca^{2+} -induced assemblies exhibit relatively sharp peaks whose magnitudes decay very slowly with q_x (Fig. S1). This slow decay of $S(q_x)$ is characteristic of the sticky rod model and is found to be essential for reproducing the data. The good agreement between the data and the sticky fluid model suggests that the overall inter-particle potential for lipid-bound TMVs includes a short-range attraction. We previously speculated that this inter-TMV attraction was counter-ion-mediated in origin [10]. This interpretation is indirectly supported in the present study by the observed insensitivity of the Ca^{2+} -induced TMV assemblies to the cationic lipid concentration. It should be noted that similar observations were previously reported for multi-lamellar DNA–cationic lipid complexes, for which high concentrations of divalent cations were found to induce close packing in 2D arrays of parallel DNA rods [35]. In that study, the spacing between condensed DNAs was also found to be independent of the cationic lipid concentration, and this behavior was interpreted as evidence for an inter-DNA attraction that was mediated by correlations between the DNA-bound divalent cations. Therefore, the similarities between the two systems suggest that an analogous Ca^{2+} -mediated attraction may exist in the 2D arrays of close-packed TMVs. The origin of the inter-TMV attraction is discussed further in Section 3 below.

3.3. Ca^{2+} concentration effect and nature of Ca^{2+} -induced attraction between TMVs

In order to gain further insights into the effects of Ca^{2+} on inter-TMV interactions, we probed the structure of TMV assemblies at

intermediate Ca^{2+} concentrations of 25 mM and 50 mM. At Ca^{2+} concentrations above 150 mM, aggregates of TMVs formed in the bulk solution (see Fig. S5 in Supporting information). The in-plane scattering profiles obtained for 0, 25, 50, and 100 mM Ca^{2+} are compared in Fig. 5 for two lipid compositions. In both cases, the in-plane correlation peaks shifted to higher q_r values as the Ca^{2+} concentration was increased, suggesting a decrease of the average inter-rod spacing.

These results reinforce the conclusion from Section 2 that the Ca^{2+} ions screen the electrostatic repulsion and induce attraction between TMVs. Fig. 5C shows that the presence of Ca^{2+} ions significantly reduces the range of repulsion between TMVs. As the Ca^{2+} concentration is increased from 25 mM ($\kappa^{-1} = 1.2$ nm) to 100 mM ($\kappa^{-1} = 0.6$ nm), the best-fit value of σ decreases from ~ 20.6 nm to ~ 19.0 nm, for both $X_{\text{TAP}} = 0.048$ and 0.3. This agreement between the two values of X_{TAP} suggests that the Coulomb repulsion between TMVs is screened mainly by Ca^{2+} ions and not by the cationic lipids when the Ca^{2+} concentration is higher than 25 mM. On the other hand, as the Ca^{2+} concentration is raised from 0 to 100 mM, η/σ increases by a factor of ~ 2 , more or less monotonically. The difference between the η/σ values for the two lipid compositions again vanishes at high Ca^{2+} concentrations (≥ 50 mM), suggesting dominant Ca^{2+} -induced attraction. In order to distinguish whether the primary role of Ca^{2+} in inducing close-packed structures is to mediate attraction or to screen repulsion, and to understand the origin of the Ca^{2+} -induced attraction between TMVs, we performed the following additional experiments.

3.3.1. Screening alone cannot induce ordered TMV assemblies

We prepared TMV samples following the procedures described in Section 1 for three lipid compositions: $X_{\text{TAP}} = 0.6, 0.8,$ and 1.0. After allowing TMV assemblies to develop for ~ 12 h and GISAXS patterns (Fig. 6A) confirmed the formation of TMV assemblies, we rinsed the sample cell with the Ca^{2+} -free buffer several times to remove the excess TMVs in the solution. We then added a small amount of concentrated Ca^{2+} solution to the remaining solution to achieve the final Ca^{2+} concentration of ~ 100 mM. After another 12 h of incubation, GISAXS patterns were again recorded (Fig. 6A and B). The corresponding best-fit values of η/σ are plotted in Fig. 6C.

For all three lipid compositions probed, the addition of Ca^{2+} resulted in substantial changes in the GISAXS patterns. The in-plane

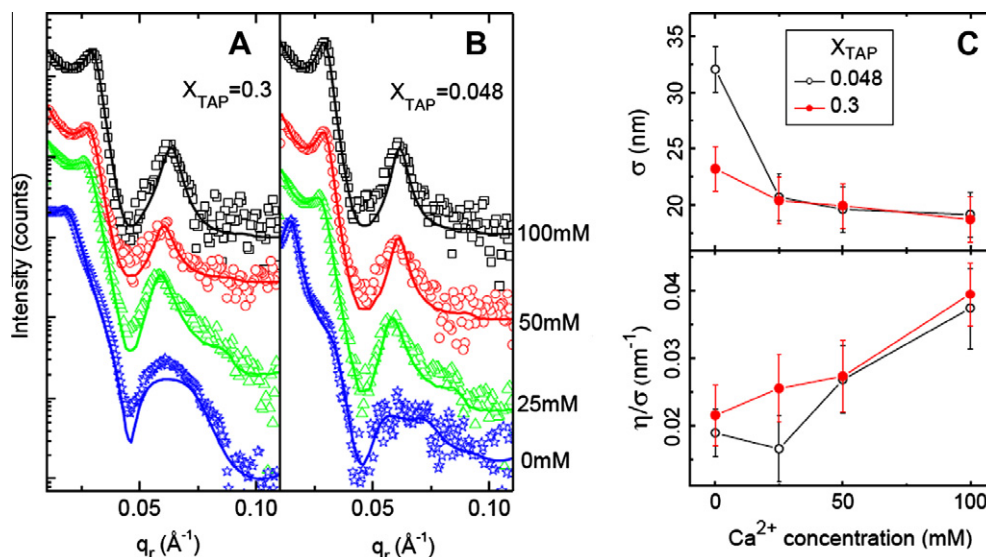


Fig. 5. In-plane scattering profiles from TMV assemblies adsorbed to lipid monolayers with $X_{\text{TAP}} = 0.3$ (A) and 0.048 (B), respectively, under MES buffers containing 100 mM (squares), 50 mM (circles), 25 mM (triangles) and 0 mM (stars) Ca^{2+} . The data are shifted vertically for clarity. The solid lines are the best-fits based on the hard rod model for the Ca^{2+} -free case and the sticky rod model for the non-zero Ca^{2+} concentrations. The corresponding best-fit values for the radius of hard-wall potential σ and the packing density of rods η/σ are shown in (C).

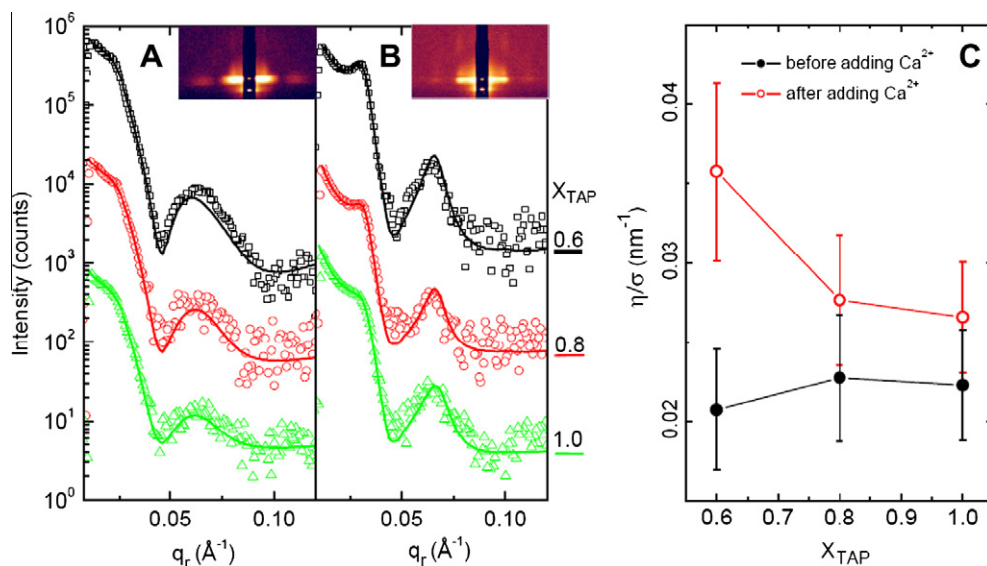


Fig. 6. The in-plane scattering profiles from three samples with $X_{\text{TAP}} = 0.6$ (squares), 0.8 (circles), and 1.0 (triangles) (A) on the lipid monolayers under a Ca^{2+} -free MES buffer, and (B) from the same samples at 12 h after increasing Ca^{2+} concentration to 100 mM. The insets are GISAXS patterns from the sample with the $X_{\text{TAP}} = 0.6$ lipid monolayer. Solid lines are the best fits, with the best-fit packing density η/σ plotted in (C). Note that the best-fit parameters for the data collected after increasing the Ca^{2+} concentration are different from those presented in Fig. 2C for samples with the same final Ca^{2+} concentration. This is most likely because in the present case the overall density of adsorbed TMVs is lower, without free TMVs to be adsorbed after the increase in Ca^{2+} concentration.

correlation peaks became more prominent and sharper, indicating that the TMV arrays became better ordered. The q_r positions of the first- and second-order peaks (0.032 \AA^{-1} and 0.064 \AA^{-1}) that developed after the addition of Ca^{2+} are almost independent of the lipid compositions (Fig. 6B) and correspond to an average spacing of $\sim 20 \text{ nm}$ between TMVs. Given the AFM-derived spacing of 32–35 nm before adding Ca^{2+} (Section 1), the Ca^{2+} -induced reduction in the inter-TMV spacing was 12–15 nm ($\sim 40\%$). These results demonstrate that the Ca^{2+} -induced close packing of lipid-bound TMVs is brought about by an attractive inter-TMV interaction. Had the added Ca^{2+} ions only screened the electrostatic repulsion between TMVs without introducing attraction, the packing density in the TMV assemblies (or average spacing between TMVs) would have remained the same because the solution contained no excess TMVs to adsorb to the lipid monolayer.

3.3.2. Attraction between TMVs has a contribution that depends on counter-ion valence

As pointed out earlier (Section 2), the success of the sticky rod model in describing the Ca^{2+} -induced structure strongly suggests that short-range attractive forces must exist between the lipid-bound TMVs to facilitate the formation of close-packed assemblies. The most probable inter-rod spacing is determined by the balance between the repulsive and attractive inter-particle forces. Once the repulsive contribution is reduced by more effective screening of the surface charges on TMVs, the attractive contribution is expected to draw the TMV rods closer together in the assemblies. This attractive force between like-charged TMVs should partly arise from the van der Waals interaction, which is thought to be responsible for the attraction between colloid particles in solution [36,37] as well as the formation of TMV bundles in bulk solutions at high ionic strength [15]. As previously discussed in Ref. [10], part of the attraction could also be mediated by counter-ions, which is also believed to be responsible for the lateral aggregation of charged rods, such as DNAs [35] and other filamentous viruses [38], under high concentrations of divalent cations. While counter-ion-mediated attraction is expected to depend on the valence of the counter-ion, the van der Waals force is not. We therefore

examined the effect of the cation valence on the structure of TMV assemblies.

We prepared TMV samples for two lipid compositions, $X_{\text{TAP}} = 0.3$ and 0.048, under pH 6.0, 10 mM MES solutions containing 300 mM NaCl, which have the same ionic strength as the 100 mM CaCl_2 solution. The final scattering patterns (Fig. 7) showed clear scattering peaks indicating in-plane ordering. The in-plane scattering data are well described by the sticky rod model, suggesting that attractive forces also exist between TMVs in the presence of Na^+ ions. However, the extracted hard-wall radius of $\sim 22 \text{ nm}$ is significantly larger than the value of $\sim 19 \text{ nm}$ obtained for Ca^{2+} -induced structures (Section 2). Moreover, the extracted stickiness parameter (see Experimental and Ref. [10]) of $\alpha \sim 0.3$ for Na^+ is significantly lower than the average value of $\alpha \sim 1$ for Ca^{2+} . Therefore, the van der Waals force, which is expected to be independent of the type of cations in the solution, cannot solely account for the entire attraction between TMVs in the presence of Ca^{2+} ions.

On the other hand, the counter-ion-mediated attraction between charged rods is thought to arise from density fluctuation in the counter-ions that are condensed on the rods [23]. The condensation of counter-ions is expected to occur when the linear charge density on the rod is sufficiently high that the electrostatic potential energy overcomes entropy [23]. The rod's linear charge density is often measured by the unitless parameter $\xi = l_b/b$, where l_b is the Bjerrum length and b is the length of the rod per unit charge. Counter-ion condensation occurs when ξ exceeds a critical value ξ_c . The resulting condensation then normalizes the nominal linear charge density so that $\xi = \xi_c$. For ideal cylinders [39], ξ_c scales with $1/z$, where z is the valence of the counter-ions. Therefore, counter-ion condensation is more likely to occur for ions of higher valence, resulting in a lower renormalized linear charge density on the rod, and consequently weaker electrostatic inter-rod repulsion and stronger attraction that is mediated by the density fluctuations in the condensed counter-ions. This expected trend is consistent with our observation that Ca^{2+} ions introduce stronger attraction between TMVs than Na^+ ions do, suggesting that counter-ion-induced attraction does play a role in the formation of TMV assemblies in the presence of Ca^{2+} ions.

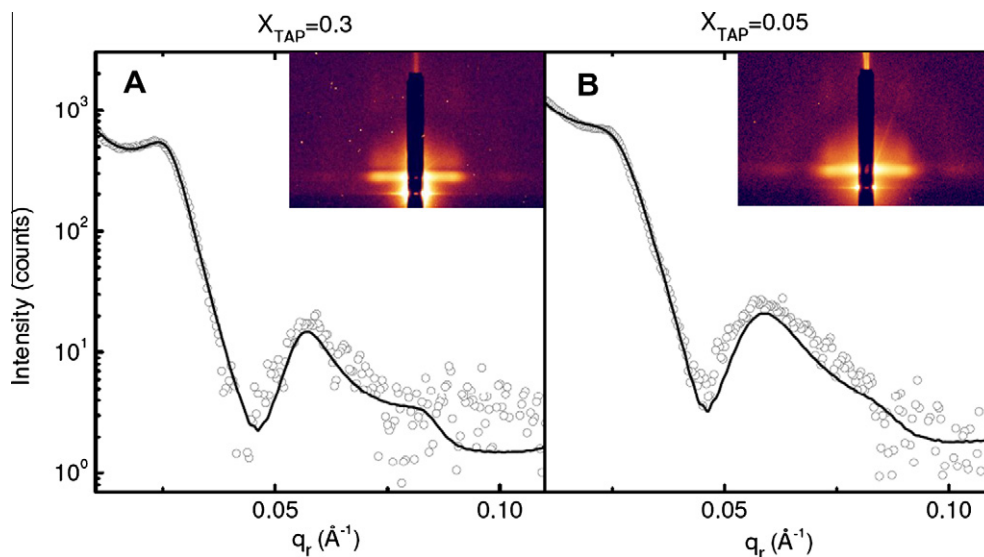


Fig. 7. In-plane scattering profiles from the final GISAXS pattern (inset) of two samples with (A) $X_{\text{TAP}} = 0.3$ and (B) $X_{\text{TAP}} = 0.05$ under pH 6.0, 10 mM MES solutions containing 300 mM NaCl. The open circles are the data. The solid lines are the best-fits using the sticky rod model.

4. Conclusion

We have studied the structure of 2D assemblies of TMVs adsorbed on lipid monolayers of DOPC/DOTAP mixtures at various mole fractions of the cationic DOTAP and under buffer solutions containing different types and concentrations of cations. These factors influence the electrostatic interaction between TMVs as well as that between TMV and the lipid monolayer, which in turn impact both the behavior of TMV adsorption onto the lipid monolayer and the final structure of the TMV assemblies.

In general, the 2D assembly of TMVs is found to be slower under solutions of higher ionic strengths, which can be attributed to screening of the electrostatic attraction between the TMVs and the lipid monolayer. At low ionic strength (10 mM MES only), the reduced screening causes the assembly to occur more quickly. Under these low-salt conditions, increasing the fractions of cationic lipids in the monolayer resulted in poorer structural order. This observation can be attributed to accelerated adsorption of TMVs at high lipid-charge densities, which we interpret as the consequence of higher surface potential at the lipid monolayer. Besides the disordering effect, higher DOTAP concentration in the lipid monolayer also resulted in higher TMV packing density, possibly due to the partial screening of electrostatic repulsion between adsorbed TMVs by mobile counter-ions within the lipid monolayer (i.e. DOTAP). Modification of the interaction between adsorbed TMVs by the ions in the bulk solution was found to dramatically affect the TMV assemblies, yielding denser and better-ordered structures with increasing concentration of Ca^{2+} ions. The improved structural order may be attributed to increased screening of the Coulomb repulsion as well as counter-ion-induced attraction between TMVs.

Our results revealed the complexity of the electrostatic interactions that are involved in the 2D assemblies of TMVs on oppositely charged lipid monolayers. While we were able to resort to simplified models to quantify the final structure in the TMV assemblies, the initial behavior of TMV adsorption cannot be inferred from the X-ray scattering data because ordered assemblies have already formed by the time the scattering intensity is sufficiently high to be analyzed. The 1D liquid model used in our data analysis should also break down when the TMVs have not yet formed large, ordered domains. Our data cannot answer definitively whether the attractive interaction between TMVs in the presence of divalent

cations is due to the condensation of these ions onto the TMVs. Nevertheless, our results provide strong evidence that the inter-TMV attraction has a component that depends on the counterion valence. The role of counter-ion condensation may be further clarified by X-ray scattering measurements from TMVs in bulk solution in the presence of high Z counter-ions.

Acknowledgments

We thank S. Kewalramani for helpful comments. The BNL contribution to this work, including use of the National Synchrotron Light Source, was supported by the US Department of Energy, Office of Basic Energy Sciences, Division of Materials Sciences and Engineering, under Contract No. DE-AC02-98CH10886. QW acknowledges the financial support from National Science Foundation under Contract No. CHE-0748690, Department of Defense under Contract No. WN11NF-09-1-236, Department of Energy, Office of Basic Energy Sciences, under Contract No. DE-SC0001477, and the W.M. Keck Foundation.

Appendix A. Supplementary material

Supplementary data associated with this article can be found, in the online version, at [doi:10.1016/j.jcis.2011.03.048](https://doi.org/10.1016/j.jcis.2011.03.048).

References

- [1] G.M. Whitesides, M. Boncheva, Proc. Natl. Acad. Sci. U. S. A. 99 (2002) 4769.
- [2] G.M. Whitesides, B. Grzybowski, Science 295 (2002) 2418.
- [3] N.D. Denkov, O.D. Velev, P.A. Kralchevsky, I.B. Ivanov, H. Yoshimura, K. Nagayama, Nature 361 (1993) 26.
- [4] N. Bowden, I.S. Choi, B.A. Grzybowski, G.M. Whitesides, J. Am. Chem. Soc. 121 (1999) 5373.
- [5] J. Zhang, X.M. Lin, M. Sprung, S. Narayanan, J. Wang, Nano Lett. 10 (2010) 799.
- [6] Y. Mao, M.E. Cates, H.N.W. Lekkerkerker, Physica A 222 (1995) 10.
- [7] A. Kulkarni, C. Zukoski, J. Cryst. Growth 232 (2001) 156.
- [8] D. Nykypanchuk, M.M. Maye, D. van der Lelie, O. Gang, Nature 451 (2008) 549.
- [9] S.Y. Park, A.K.R. Lytton-Jean, B. Lee, S. Weigand, G.C. Schatz, C.A. Mirkin, Nature 451 (2008) 553.
- [10] L. Yang, S.T. Wang, M. Fukuto, A. Checco, Z. Niu, Q. Wang, Soft Matter 5 (2009) 4951.
- [11] M.S. Wertheim, J. Math. Phys. 5 (1964) 643.
- [12] E. Leutheusser, Physica A 127 (1984) 667.
- [13] S.B. Yuste, A. Santos, J. Stat. Phys. 72 (1993) 703.
- [14] S. Kewalramani, S.T. Wang, Y. Lin, H.G. Nguyen, Q. Wang, M. Fukuto, L. Yang, Soft Matter 7 (2011) 939.

- [15] B.M. Millman, T.C. Irving, B.G. Nickel, M.E. Loosley-Millman, *Biophys. J.* 45 (1984) 551.
- [16] D.J. Needleman, M.A. Ojeda-Lopez, U. Raviv, H.P. Miller, L. Wilson, C.R. Safinya, *Proc. Natl. Acad. Sci. U. S. A.* 101 (2004) 16099.
- [17] G.C.L. Wong, L. Pollack, *Annu. Rev. Phys. Chem.* 61 (2010) 171.
- [18] S.T. Wang, M. Fukuto, L. Yang, *Phys. Rev. E* 77 (2008) 031909.
- [19] N. Kucerka, J.F. Nagle, J.N. Sachs, S.E. Feller, J. Pencer, A. Jackson, J. Katsaras, *Biophys. J.* 95 (2008) 2356.
- [20] I. Watanabe, N. Ui, *Bull. Chem. Soc. Jpn.* 29 (1956) 345.
- [21] C. Shew, A. Yethiraj, *J. Chem. Phys.* 106 (1997) 5706.
- [22] R. Menes, N. Gronbech-Jensen, P.A. Pincus, *Eur. Phys. J. E* 1 (2000) 345.
- [23] W.M. Gelbart, R.F. Bruinsma, P.A. Pincus, V.A. Parsegian, *Phys. Today* 53 (2000) 38.
- [24] K. Wagner, D. Harries, S. May, V. Kahl, J.O. Radler, A. Ben-Shaul, *Langmuir* 16 (2000) 303.
- [25] J. Radler, I. Koltover, T. Salditt, C.R. Safinya, *Science* 275 (1997) 810.
- [26] I. Koltover, T. Salditt, C.R. Safinya, *Biophys. J.* 77 (1999) 915.
- [27] L. Yang, H. Liang, T.E. Angelini, J. Butler, R. Coridan, J.X. Tang, G.C.L. Wong, *Nat. Mater.* 3 (2004) 615.
- [28] T. Salditt, I. Koltover, J.O. Radler, C.R. Safinya, *Phys. Rev. Lett.* 79 (1997) 2582.
- [29] I. Koltover, S. Sahu, N. Davis, *Angew. Chem., Int. Ed.* 43 (2004) 4034.
- [30] H. Clausen-Schaumann, H.E. Gaub, *Langmuir* 15 (1999) 8246.
- [31] A. Gromer, M. Rawiso, M. Maaloum, *Langmuir* 24 (2008) 8950.
- [32] J.N. Israelachvili, *Intermolecular and Surface Forces*, second ed., Academic, San Diego, 1992.
- [33] R. Richter, A. Mukhopadhyay, A. Brisson, *Biophys. J.* 85 (2003) 3035.
- [34] J. Seelig, *Cell Biol. Int. Rep.* 14 (1990) 353.
- [35] I. Koltover, K. Wagner, C.R. Safinya, *Proc. Natl. Acad. Sci. U. S. A.* 97 (2000) 14046.
- [36] D.G. Grier, *Nature* 393 (1998) 621.
- [37] F. Bresme, M. Oettel, *J. Phys. Condens. Matter* 19 (2007) 413101.
- [38] J.X. Tang, P.A. Janmey, A. Lyubartsev, L. Nordenskiöld, *Biophys. J.* 83 (2002) 566.
- [39] G.S. Manning, *J. Phys. Chem. B* 111 (2007) 8554.